

Top Partners at the LHC: Spin and Mass Measurement

Patrick Meade and Matthew Reece

*Institute for High Energy Phenomenology
Newman Laboratory of Elementary Particle Physics
Cornell University, Ithaca, NY 14853, USA*

meade, mreece@lepp.cornell.edu

Abstract

If one takes naturalness seriously and also assumes a weakly coupled extension of the Standard Model (SM) then there are predictions for phenomenology that can be inferred in a model independent framework. The first such prediction is that there must be some colored particle with mass $\mathcal{O}(\text{TeV})$ that cancels the top loop contribution to the quadratic divergence of the Higgs mass. In this paper we begin a model independent analysis of the phenomenology of this “top partner,” t' . We make one additional assumption that it is odd under a parity which is responsible for the stability of a WIMP dark matter candidate, N . We focus on three questions to be explored at the LHC: discovery opportunities, mass determination, and spin determination of this top partner. We find that within a certain region of masses for the t' and N , $t'\bar{t}'$ is easily discovered in the $t\bar{t} + 2N$ decay with the tops decaying fully hadronically. We show that without having to rely on other channels for new physics that for a given t' spin the masses of t' and N can be measured using kinematic information (e.g. average E_T or H_T) and total cross section. A degeneracy due to the spin remains, but with several hundred fb^{-1} of luminosity we demonstrate potentially useful new methods for determining the t' spin over a wide range of masses. Our methods when could be useful for distinguishing supersymmetric and non-supersymmetric models.

1 Introduction

In building models of physics beyond the Standard Model (SM), naturalness has been a key motivating guideline. The Higgs boson of the SM receives radiative corrections to its mass from loop diagrams involving SM particles. These corrections are quadratically divergent, implying that either new physics cancels them (naturalness) *or* the bare mass of the Higgs is finely-tuned. The canonical example of weakly coupled natural new physics is supersymmetry, in which the quadratic divergences are cancelled by superpartners of known particles having spins differing by $1/2$. However, in recent years there have been many new ideas for implementing naturalness in a weakly coupled framework (at least at the TeV scale), among them little Higgs models [1].

Experimental consequences of models implementing naturalness have been explored to some extent, but the space of possible models is large. The space of models is also augmented by the fact that a given model (for instance the MSSM) can also have a large set of freely chosen parameters. Since the space of models and their parameters is so large, many phenomenological studies can become mired in the model dependent consequences of a particular implementation of new physics. In this paper we advocate an alternative direction: we wish to explore *model independent* LHC phenomenology motivated by naturalness. This allows us to focus in on key signatures that can be motivated from naturalness without becoming stuck in the framework of a particular model. Additionally we focus only on the LHC to investigate how much physics information can be gleaned from its results alone, independent of the abilities, or lack thereof, of any future machine.

We begin by looking at the key ingredients in a natural extension of the SM. Assuming that an SM-like Higgs exists and physics beyond the SM is weakly coupled at the TeV scale, the first expectation from naturalness is an enlarged “top sector.” The top loop in the SM is the largest contribution to the Higgs mass quadratic divergence. Thus there must be some new particle(s) constrained by symmetry to have couplings related to those of the top, which cancel this loop. For instance in supersymmetry there are scalar tops (“stops”). In Little Higgs theories there are fermionic top partners. We call the generic top partner t' . One could continue adding new particles based on naturalness, such as partners of the gauge bosons and Higgs, but we will focus now solely on the top sector.

We assume that the t' that cancels the top loop is in the fundamental representation of $SU(3)$, as in all examples we are aware of, so that some symmetry can relate it to the t . Thus the t' couples to gluons and will be produced at the LHC in the processes $gg \rightarrow t'\bar{t}'$ and $q\bar{q} \rightarrow t'\bar{t}'$. Assuming no new particles or in scenarios where the t' decays to other particles beyond the SM but no stable new particle exists, the resulting decay of the t' will then solely end in SM particles. Such SM decay modes will be relatively easy to find at the LHC, as one can apply various cuts and build invariant masses to find a resonance (similarly to how the top itself is studied.)

On the other hand, if one has decays to SM particles plus a stable neutral invisible particle (as in SUSY), the situation is much more challenging. With a stable invisible particle escaping detection one cannot simply construct invariant masses. On the other hand, requiring large \cancel{E}_T can dramatically cut back Standard Model backgrounds. This scenario

is also well-motivated both from providing a dark matter candidate and from various precision constraints. In typical models of physics beyond the SM, four-fermion operators or electroweak oblique corrections are too large without a parity forbidding the largest contributions. Therefore beyond naturalness we will further assume, for now, that there is some conserved \mathbb{Z}_2 parity. Examples include R-parity [2](or Matter Parity [3]), T-parity [4], and KK-parity [5]. The lightest particle charged under this parity is stable. We will call the stable particle the LPOP (“lightest parity-odd particle”), since we do not assume a particular model for the parity.

For this paper we focus on a minimal scenario which is very plausible for the LHC (if naturalness has any role in TeV scale physics): there is some parity-odd heavy top t' , of undetermined spin, decaying to the usual top quark t and the LPOP N . Because of the odd parity we must pair-produce the t' , so the collider signature will be $t\bar{t} + \cancel{E}_T$. Of course, a truly model-independent approach would have undetermined couplings for every decay of the t' that does not violate a symmetry, so we would also consider, for instance, $t' \rightarrow cN$ or $t' \rightarrow be^+\nu_e N$ (without the constraint $m_{be\nu} = m_t$, e.g. through a W'). However, in most particular models the $t' \rightarrow tN$ decay is dominant, or at least large. Since the t' and t are closely related this is not surprising. Hence we consider only the minimal scenario with decay $t' \rightarrow tN$. As we will discuss, even when other decay modes are available, the approach we outline can still be useful.

We should stress that we do *not* have particular models in mind. We work from minimal effective Lagrangians that display a signature that could be seen in any number of models (perhaps even unnatural ones). Our study is *signature based*: we build very general effective Lagrangians that generate $t\bar{t} + \cancel{E}_T$, under the assumption that it arises from $t't' \rightarrow t\bar{t} + 2N$, and focus on pinning down properties of the new particles at the LHC. Part of our motivation for such a study is provided by the observation that certain models, like universal extra dimensions [6] or little Higgs models with T-parity [7, 8], can to some extent “fake” supersymmetric spectra unless one can measure spins. Some recent papers have addressed how to distinguish spins/models in particular cascade decays [9–12]. We think that more studies along these lines are important for having a realistic sense of how well the LHC can discriminate among models and for building a preliminary toolkit of ideas and techniques for analysis. Another motivation is that it is quite plausible the correct model of TeV scale physics has not yet been written down but nevertheless naturalness could be a key ingredient in how nature works. By parameterizing one of the most logical possibilities for naturalness in terms of these minimal effective lagrangians we can still analyze the possibilities and develop new techniques for the LHC without requiring all the details of nature’s choice for the TeV scale.

In this paper we attempt to answer the following questions:

- Can the signature be observed at high significance over the SM backgrounds?
- How well can we determine the masses of the t' and N ?
- Can we devise an algorithm for measuring the spin of the t' or the N ?

As we will show, with several years of high-luminosity running all of these except perhaps the spin determination for the N should be possible at the LHC. In the all-hadronic decay mode, a high signal-to-background ratio can be achieved over a wide range of masses. Kinematic variables like average \bar{E}_T or H_T (see Sec.3.1 for definitions) give some indication of the mass splitting between the t' and N , while the total cross section determines the t' mass for a given spin of t' . This leaves a degeneracy. For the same cross section and kinematic averages, the case of scalar t' has a lower mass and so a higher overall boost. We show that this allows pseudorapidity distributions of the t and \bar{t} to be used, given enough luminosity, to determine the t' spin for a wide range of masses.

The rest of the paper is organized in the following way. In Section 2 we set up the details of the model independent framework that we analyze as well as giving examples of existing models included within our setup. In Section 3 we examine the discovery possibilities for the signal at the LHC. In Section 4 we analyze the possibilities of mass determination and point out a degeneracy due to spin that is often overlooked. We then attack the issue of spin determination in Section 5 where we present new asymmetries and we use pseudorapidity correlations to determine the spin of the t' . We then discuss in section 6 the impact of our model independent study when considered in the context of existing models. We conclude by discussing future research directions for this comparatively rare type of model independent analysis.

2 Model Independent Framework

In this section, we wish to set up the framework for what we study. We are trying to address the question of what is a reasonable first signature of new physics at the LHC in a model independent manner, but we must construct some effective Lagrangian to work with. We have established that our particle content is a heavy top partner t' and the LPOP N with a decay $t' \rightarrow tN$. In principle we could fix the quantum numbers of the t' by investigating every possible mechanism of cancelling the quadratic divergence of the top quark in the SM. While this would allow for a completely model independent study there presumably could always be a loophole for the cancellation that we have missed. There are many existing models with top partners that cancel (at least to one loop) the quadratically divergent contribution of the top quark to the Higgs mass, for instance SUSY or Little Higgs. What we find from this is that there are two reasonable possibilities for the top partner spin: it could be either a spin 1/2 fermion or a scalar ¹. While this may be viewed as introducing some model dependence we will *not* restrict ourselves to the parameters in these models. The spins implied by the various existing mechanisms for naturalness are only used as a possible starting point.

Once the spin of the t' is fixed, the vertex for the decay $t' \rightarrow tN$ fixes the possible spins of the N . In the case that the t' is a scalar N must be a fermion. On the other hand if the t' is a fermion it implies that N could either be a scalar, spin 0, or vector, spin 1, particle.

¹More exotic possibilities could perhaps occur if there were some composite resonance but we will avoid these cases since there isn't an obvious symmetry to relate the couplings. In this paper for the spins of the particles we will restrict ourselves to the case of spin 1 and less.

At this point we need a way to fix the SM gauge quantum numbers of the t' and N . As was mentioned before we have already demanded that the t' is in the fundamental representation of $SU(3)$. However, the electroweak quantum numbers have not been fixed. Since the LPOP is a neutral stable particle the vertex $t'tN$ also fixes the electric charge of the t' to be the same as the top quark. Hence we only must determine the representation of $SU(2)$ that the t' candidate resides in. This could in principle be fixed by examining the various mechanisms for cancelling the quadratic divergences of the Higgs mass and what the vertex with the Higgs implies for the $SU(2)$ quantum numbers. Generically in existing models there are cases where there are top partners which can be both singlets and doublets of $SU(2)$. Since we are trying to present a new framework for studying physics beyond the SM, to limit the scope of our study we will only analyze the case where both the t' and N are singlets of $SU(2)$. This does not mean we assume there are no doublets, merely that they are heavy enough and with small enough mixing that they do not influence the results. This choice avoids the issues of introducing a partner of the bottom quark or additional particles associated with the N (for instance charginos or other gauge bosons). In Section 6 we will further discuss the issues relevant to our study created from introducing new particles.

We now summarize the particle content for our study: a singlet t' which is either a scalar or fermion with mass $m_{t'}$, and the LPOP singlet N , with mass m_N , which is a fermion in the case of a scalar t' and a scalar or vector in the case of a fermionic t' . Because of our assumptions the coupling to the SM top quark takes the form

$$\mathcal{L}_{t'tN} \sim g_{t'N}(t'\bar{t}_RN + h.c.). \quad (2.1)$$

In principle we could relax the assumption of having only a light singlet t' and it could mix with a heavier doublet partner of the top leading to a coupling of the form

$$\mathcal{L}_{t'tN} \sim t'\bar{t}(g_{t'N_L}P_L + g_{t'N_R}P_R)N + h.c., \quad (2.2)$$

where $P_{L,R} = (1 \pm \gamma_5)/2$ and we have omitted the details of the Lorentz structure that depend on the spins of t' and N . This resembles more closely the situation in SUSY where \tilde{t}_L and \tilde{t}_R mix to form \tilde{t}_1 and \tilde{t}_2 . So as not to complicate our scenario any further we will assume that the coupling is of the form (2.1). We will discuss the effects of this assumption in Sections 4 and 5. Thus for our study there will naively be three parameters separate from the choice of spin, $m_{t'}$, m_N , and $g_{t'N}$. Since the t' only has one decay channel available to it, calculating its decay width properly means that $g_{t'N}$ is not actually an additional parameter in our study (except for small interference effects, important only when $m_{t'} \approx m_t + m_N$).

2.1 Model Dependent Realizations

So far we have presented a model independent realization of what one would expect from naturalness supplemented by a parity with a neutral LPOP. This realization is only a subset of possibilities for a top partner but nevertheless a sensible starting point. It is important to note that this model independent framework that we have laid out can also realize many existing models of physics beyond the SM. In most of the cases that we will discuss there

are additional other particles beyond our minimal set and their impact will be discussed in Section 6.

The case of a scalar t' is obviously analogous to a stop in the MSSM. For our particular choice of quantum numbers the scenario in the MSSM would correspond to t' being a light \tilde{t}_1 that was predominantly \tilde{t}_R , while the N would correspond to the lightest neutralino, χ_1^0 , being mostly Bino and the LSP (LPOP). A particular realization where these are the lightest new particles in the MSSM is not the most common region of parameter space. However, it is a relatively typical region of parameter space in mSUGRA to have the \tilde{t}_R being the lightest colored particle and a Bino-like LSP. While there may be other particles in the same mass range relevant to the LHC, the decay $\tilde{t}_1 \rightarrow t\chi_1^0$ typically has a sizeable branching fraction.

Having a fermionic t' cancel the quadratic divergence to the Higgs mass from the t occurs within the framework of Little Higgs models [1]. However since we are only interested in the case of a parity odd t' the relevant models are those with a T-parity [4]. In the original models of Little Higgs with T-parity the cancellation of the top loop divergence in the SM was due to a parity even top quark partner but in addition there was always a T-odd partner t'_- which is lighter [7]. The decay of the t'_- in the Littlest Higgs with T-parity has only one channel $t'_- \rightarrow tA_H$ where A_H is the LTP (LPOP), a heavy partner of the hypercharge gauge boson of the SM (up to small v/f -suppressed mixings). This is the case of a t' fermion and N vector that we have laid out. In addition there has been a recent paper [8] where the t'_- was responsible for cancelling the divergence to the Higgs mass, which is also directly realized in our framework.

The examples of specific models contained within our model independent realization given so far, not surprisingly, are guided by the assumption of naturalness. However within our naturalness motivated model independent framework it is also interesting to note that we can accommodate models that do not necessarily address the question of naturalness. An example of this type is UED [5] models, which have received considerable attention as an example of a model which can be confused with SUSY [6]. In these models the SM propagates into an extra dimension(s) and thereby KK partners of all SM particles exist. These models have a discrete symmetry, KK-parity, that provides an LKP (LPOP) that is typically the KK partner of the photon. Therefore in these types of models the KK partner of the top quark t_{1R} decays to t_R and the LKP A_1 , and so is also realized within our framework.

From the above examples we see that the model independent realization we have chosen can obviously be applied to a host of existing models. Of course the caveat exists that in many models there will be other non-SM backgrounds that would need to be taken into account which will be discussed in Section 6. Notwithstanding the particular examples of our framework containing existing models, we reiterate that this framework is not simply model inclusive but model independent. The parameters of our study $m_{t'}$ and m_N are usually fixed in all examples that we have given so far based on other parameters in the given model. In our study $m_{t'}$ and m_N will be varied freely within a certain range that *can not necessarily* be realized in the above examples. We thus look for the signature $t\bar{t} + \cancel{E}_T$ in regions that would not necessarily be accessible by the models existing so far, hence the distinction model independent.

3 Discovery Opportunities

In this section we will examine the discovery opportunities for the signal $t\bar{t} + 2N$ where the N is neutral LPOP that escapes the detector. Our signal has several possible channels that we could look at depending upon how the W gauge bosons from the top end up decaying. Comparing the leptonic or semileptonic channels versus the hadronic channel, we see that in a leptonic channel there is already a source of \cancel{E}_T (from neutrino(s)) in the SM while in the hadronic channel there is no SM contribution to the \cancel{E}_T . Thus the largest SM irreducible background in the leptonic case would be $t\bar{t}$ while for the hadronic channel it would be $t\bar{t}Z$ where $Z \rightarrow \nu\bar{\nu}$ ¹. Therefore the backgrounds are much smaller in the hadronic channels than in the semileptonic channel. It is also important to note that not only are the backgrounds smaller in the hadronic channel, there is more kinematic information as well. In the leptonic channels the additional source of \cancel{E}_T from the neutrinos reduces the amount of kinematic information about the original $t\bar{t}$ pair, whereas in the hadronic channel the momenta of the top quarks can be fully reconstructed. For these reasons we will focus on the hadronic channel for our signal.

To study this signal we implement the effective framework discussed in Section 2 using the MadGraph software [13]. The coupling $g_{t'N}$ in (2.1) was set to the electric charge e . However, as discussed in Section 2, this coupling is not really a free parameter since we have assumed there is only one decay channel. Since we have assumed that the t' is in the fundamental representation of $SU(3)$ we implement a single gluon coupling for a fermionic t' and both a single and double gluon vertex for the scalar t' . In calculating all processes that contribute to $t\bar{t} + 2N$ we use the parton distribution function CTEQ6L1 [14]. The renormalization and factorization scales used for our signal will be the mass of t' . The factorization and renormalization scale dependence of our results could be minimized by calculating the effects beyond leading order, but for now we refer to the NLO QCD corrections to $t\bar{t}$ production where m_t is a reasonable choice of scale [15]. It is important to note that MadGraph is only a tree level matrix element generator. For our study we will compare tree level signal and background cross sections. The QCD corrections will tend to increase both our signal and background as well as pin down the factorization and renormalization scales. This increase should be an order one effect and could be absorbed into a K-factor but will not affect our results in any qualitative manner in the bulk of our parameter space. Future studies taking into account more detailed issues could investigate this further but it is a reasonable starting point to compare tree level signal and background to come up with new techniques.

We will split the discussion of discovery opportunities into several parts. We will begin by giving the definitions of all kinematic variables used in our study. We then describe the cuts used in analyzing both signal and background. Before discussing the various backgrounds we will collect the efficiencies relevant to the process studied. We then give the background cross sections taking into account our cuts and the efficiencies. To demonstrate the discovery

¹There are many additional sources of backgrounds that one must consider, such as W +jets or Z +jets, different decays of a $t\bar{t}$ pair with additional jets combined with incorrect particle IDs, energy mismeasurement, and so on. It turns out after applying our cuts and taking into account various efficiency considerations the backgrounds just listed are smaller. We will give our estimates of the various backgrounds in Section 3.4.

opportunities we then look at both the usual measure of signal to root background, and then the signal to background ratio.

3.1 Definitions of Kinematic Variables

To discriminate signal from background, we wish to apply a set of kinematic cuts on certain variables. These variables also will prove useful in determining the masses of the t' and N , as we will discuss in Section 4. Here we collect the definitions of the kinematic variables we will be considering:

- $|\mathcal{E}_T|$: At the parton level we define $|\mathcal{E}_T|$ as the length of the transverse momentum vector constructed from the vector sum of transverse momenta of all neutrinos and the N 's.²
- H_T : H_T is defined as the *scalar* sum of transverse momenta of the reconstructed objects. More precisely, H_T is $|\mathcal{E}_T|$ plus the sum of $|E_T|$ for all jets, electrons, and taus, plus the sum $|p_T|$ of all muons.
- M_{eff} : M_{eff} has developed a reputation as a good measure of the mass scale of the strongly interacting particle [16, 17]. It is defined to be the sum of $|E_T|$ for the four highest- $|E_T|$ jets, plus the $|\mathcal{E}_T|$, where the distribution is only used for events satisfying certain cuts: we require $|\mathcal{E}_T| > \max(100 \text{ GeV}, 0.2M_{eff})$, the highest jet $|E_T| > 100 \text{ GeV}$, at least four jets with $|E_T| > 50 \text{ GeV}$, and no muon or isolated electron with $p_T > 20 \text{ GeV}$ and $|\eta| < 2.5$.
- $M_{T2}(m_{N;ref})$: Proposed by Lester and Summers [18], $M_{T2}(m_N)$ is a variable that would give us $m_{t'}$ if the N mass is known precisely. This works in much the same way that, for instance, the W mass can be obtained from a histogram of the transverse mass constructed from an electron and missing energy. It is a generalization of transverse mass defined as

$$M_{T2}^2 = \min_{\mathbf{p}_T^{N_1} + \mathbf{p}_T^{N_2} = \mathbf{p}_T} \left[\max \left[m_T^2(\mathbf{p}_T^{t_1}, \mathbf{p}_T^{N_1}), m_T^2(\mathbf{p}_T^{t_2}, \mathbf{p}_T^{N_2}) \right] \right], \quad (3.1)$$

where $\mathbf{p}_T^{t_1}$ and $\mathbf{p}_T^{t_2}$ are the transverse momenta of the reconstructed top quarks (or more generally, the relevant reconstructed particles), and m_T is the transverse mass of two particles defined to be valid for arbitrary masses. Then M_{T2} by construction never exceeds the mass of the heavy top, provided m_N is known. The minimization is over all ways of splitting the missing transverse momentum among the two disappearing particles. The definition can be recast in a form that requires only a one-dimensional

²In practice, one cannot define \mathcal{E}_T in this way. Instead \mathcal{E}_T is defined to be opposite to the vector constructed from summing E_T 's of all visible objects. More precisely, E_T of an object is normalized by the energy deposited in the calorimeter, and the direction is obtained from the location of the energy deposit relative to the event vertex. For muons one would use p_T , as the momentum is well-measured from the track but the muon does not deposit all of its energy in the calorimeter.

minimization, which is easier to compute. For this and other details see the original papers [18]. Since m_N is unknown as well in our case, we must be careful about the use of this variable. We supply an “input” N mass, $m_{N;ref}$, which might be quite different from the actual N mass. The histogram of $M_{T2}(m_{N;ref})$ has a lower edge determined by $m_{N;ref}$ and a fairly sharp upper edge. We denote this upper edge $M_{T2}^{max}(m_{N;ref})$. Changing the input $m_{N;ref}$ will shift the position of the edge but does not alter its existence.

3.2 Cuts

Since our signal is $t\bar{t} + \cancel{E}_T$, we clearly need to require some large amount of \cancel{E}_T to discriminate our signal from the Standard Model $t\bar{t}$ background. In this way we should be able to ensure the dominant background is $t\bar{t}Z$. Also, we have to ensure that the events we consider will pass the relevant triggers. Requiring $\cancel{E}_T > 100$ GeV and one jet with $E_T > 100$ GeV should be sufficient for this requirement [19]. We place a conservatively hard cut of 40 GeV on the E_T of all relevant jets, to help reduce QCD backgrounds and to guard against multiple interactions and initial- and final- state radiation. We demand two tagged b jets to ensure that our SM backgrounds are mostly top-related, as opposed to the much more common $W + jets$ and $Z + jets$ events. Furthermore, to be sure that we are looking at events involving $t\bar{t}$ we apply some mass reconstruction cuts.

To summarize, we use the following set of cuts:

- Two b -tagged jets and four other jets having $E_T > 40$ GeV.
- At least one jet with $E_T > 100$ GeV.
- $\cancel{E}_T > 100$ GeV.
- $|\eta| < 2.5$ for all jets.
- $\Delta R > 0.4$ between any pair of jets.
- The four non- b jets split into two pairs reconstructing to a W : $60 \text{ GeV} < M_{jj} < 100 \text{ GeV}$.
- The two W s pair up with the two b jets to reconstruct to a top: $150 \text{ GeV} < M_{j\bar{j}b} < 190 \text{ GeV}$.
- $H_T > 500$ GeV, where $H_T = \cancel{E}_T + \sum_{jets} |\mathbf{p}_T|$ (see below).

Additional cuts can be made to attempt to make a more pure sample. Additionally a more sophisticated analysis for the reconstruction of the top quark mass window candidates has been looked at in the past [20]. We believe our cuts are conservative enough though that our background estimates will be reliable. Once the mass scale for the signal is determined from methods presented in Section 4 the cuts can be tuned further to enhance the signal. Recently an analysis of the ability to measure the $t\bar{t}Z$ couplings at the LHC was made in

the $Z \rightarrow \nu\nu$ all hadronic channel using similarly conservative cuts [21]. In this study it was claimed $t\bar{t}Z$ could be seen above the SM backgrounds thus with the typically larger \cancel{E}_T of our signal it is even more likely our estimates are conservative enough or can be made even better with a larger \cancel{E}_T cut.

3.3 Efficiency Considerations

Here we will consider a few issues that are very important for us to understand how efficient we can be at identifying candidate signal events. First, how often will we tag a true b -jet, and how often will a non- b jet be tagged? It is clear that QCD multijet backgrounds can be large if we do not insist on having b jets. Second, how often will a hadronically-decaying τ lepton fake a jet, and how often will a true jet be reconstructed as a hadronically-decaying τ ? Backgrounds with $W \rightarrow \tau\nu$ can be troublesome, so we need some ability to veto them. There are, of course, other efficiencies to consider. Problems can arise from mismeasurement of energies, for instance. We will leave a detailed consideration of those difficulties to experimentalists; such issues will become much more clear when the LHC is operating. However we can make some preliminary estimates of how troublesome these effects could be.

In the case of b jets, the efficiency for tagging a true b jet in the p_T range we are looking at is claimed to be about 60% with a factor of 100 rejection for light-quark or gluon jets and a factor of 10 rejection for charm jets [17]. Thus we expect approximately a 30% efficiency for correctly b -tagging the signal. (At high luminosity running the efficiency of b -tagging is expected to decline to 50% at the same rejection.)

For τ leptons, the situation is troubling, as we have many light quark jets that can potentially reconstruct as a τ and cause us to veto good signal events. The τ decays hadronically about 64% of the time [22]. At high p_T a hadronically-decaying tau will fake a jet 5% of the time while 10% of light-quark jets will reconstruct as a τ [23]. Imposing a τ veto on all our jets will thus impose about a 60% efficiency factor. The cited study does not include separate rates for light-quark jets, charm jets, and b jets faking taus, but uses some large sample of $t\bar{t}$, $b\bar{b}$, and W +jets. It does note that b jets are less likely to fake taus than other jets. We will assume that the distribution of various types of jets in the samples studied is similar to that in our signal. We will also assume that we need not reject any b -tagged jets that fail the tau veto. We explain below that rejecting *every* event with a τ candidate may not be necessary, as we can use transverse mass information to help distinguish signal from background. Furthermore, one would like to have a τ ID likelihood that allows us a finer resolution on the extent to which a jet is tau-like. Highly tau-like jets could be cause for immediate veto, while moderately tau-like jets could be kept or not depending on other selection criteria.

To summarize, we will define $\epsilon_{b\tau}$ to be the efficiency, in a given sample, of tagging all b jets and passing a tau veto. We will give an estimate of this quantity for each sample, but such estimates are very preliminary. It is important to keep in mind that fake rates and efficiencies are dependent on flavor and on signal. When the LHC begins to operate one can gain a better understanding of the efficiencies and fake rates involved (studying the large

signal of $t\bar{t}$ in the SM will probably be useful). With all of these caveats, we estimate that for our signal, the efficiency is $\epsilon_{b\tau} \approx 18\%$.

Another consideration is mismeasurement, which can be problematic in two main ways. The first is that signal events can fall outside the mass window cuts due to poor measurement of jet energies. A good understanding of detector resolution is needed to study this. One might attempt to rescale energies in suitable candidate events so that the jj masses near the W mass are constrained to equal the W mass. A more detailed study of such possibilities is necessary. In the worst case, we lose efficiency by some factor ϵ_{recon} . ATLAS simulations of $t\bar{t}$ show a mass peak with a width of 13.4 GeV [17], so our 15 GeV window on each top could imply that we miss about half the events. However, since we require *both* tops to decay hadronically and lie in the mass window, the combinatorial background is likely to be smaller than in the semileptonic case. Further, one might impose a weaker window on one of the tops than on the other.

The second mismeasurement concern is that \cancel{E}_T can be overestimated in hadronically-decaying $t\bar{t}$ events. The $t\bar{t}$ cross section is so large that even if this happens rarely, it could still lead to backgrounds as large as the others we are considering. There are really two distinct issues here: the first is that jet energies can be mismeasured, creating \cancel{E}_T where there is none. This should not be very likely; ATLAS studies have indicated that missing E_T resolution is well-described by $\sigma_{\cancel{E}_T} = 0.46\sqrt{\sum E_T}$ at low luminosity and is twice as bad at high luminosity [17]. Thus measuring 100 GeV of \cancel{E}_T where there is none should happen rarely. The other source of \cancel{E}_T overestimation is that semileptonically decaying b jets can contain a high E_T neutrino. We have taken a first look at this, using the PGS detector simulation [24] on a sample of $t\bar{t}$ events generated with Pythia [25]. It appears that roughly 0.2% of all fully-hadronic $t\bar{t}$ events have $\cancel{E}_T > 100$ GeV. For comparison, note that $t\bar{t}Z$ has a cross section of order 0.1% that of $t\bar{t}$. Thus we can't immediately discount the $t\bar{t}$ background with \cancel{E}_T from semileptonic b decays. However, if a large fraction of the b energy goes to a neutrino, it is unlikely that the reconstructed jjb mass will lie near the top mass, so we expect the mass window cut to have much lower efficiency on the $t\bar{t}$ sample than on the $t\bar{t}Z$ sample. To get a definitive answer to this question, a study of all the backgrounds with detector simulation is necessary. We expect that after all cuts are applied it is not problematic.³ At worst it leads to an $\mathcal{O}(1)$ increase in background, which is only detrimental at the high end of the mass range we consider. If this problem proves to be much more severe than we estimate, one should still be able to cut the extra background by simply imposing a harder \cancel{E}_T cut of 150 GeV or 200 GeV. So long as $m_{t'}$ is not too close to $m_N + m_t$, this will still keep a substantial fraction of our signal events. The major drawback to using such harder cuts is that one needs more integrated luminosity to build up a clean signal sample for precision studies to determine spin.

One might also worry that our cut $\Delta R > 0.4$ between partons could be insufficient to prevent the reconstructed jets from overlapping, and that the resulting difficulty in recon-

³We are aware of a study in progress of all-hadronic physics at the LHC (specifically, of the stau coannihilation region) with similar \cancel{E}_T and E_T requirements, which also reaches the conclusion that SM $t\bar{t}$ background is low [26].

struction could cause problems. We also ran our cuts with $\Delta R > 0.7$ and find that about 30% of the $t\bar{t}Z$ background is kept. On the signal, the efficiency of this cut is highly dependent on $m_{t'}$ and m_N , but typically in the 20% to 30% range. At high $m_{t'}$ mass the S/B ratio will drop with the stricter separation requirement. For our purposes we will keep the $\Delta R > 0.4$ separation cut and assume that the jet algorithms are capable of separating overlapping jets intelligently.

With all of these various efficiency issues we have outlined above they must be revisited with a full detector simulation. We have attempted to be conservative in our estimates to give the reader confidence in the fact that a full detector simulation of our methods would be worthwhile.

3.4 Backgrounds in the All-Hadronic Channel

As we have noted, the largest background is the $t\bar{t}Z$ channel. We simulate this background with MadGraph. The quark content of this sample is the same as in the signal, so we estimate $\epsilon_{b\tau} \approx 18\%$. With the cuts listed above, we obtain⁴:

$$\sigma(t\bar{t}Z) = 0.32 \text{ fb.} \quad (3.2)$$

The next significant background to consider is $t\bar{t}j \rightarrow \tau jjj b\bar{b} + \cancel{E}_T$. Here the hadronic tau decay, together with the extra jet, can sometimes mimic the two jets from a W decay. We simulate this background with MadGraph. In this case we estimate $\epsilon_{b\tau} \approx 1.1\%$. MadGraph only includes two hadronic decay modes of the τ , namely $\tau^- \rightarrow \pi^- \nu_\tau$ and $\tau^- \rightarrow \rho^- \nu_\tau$. The ρ events pass our cuts slightly more often than the π events, but the efficiency is approximately the same. We will estimate that the other hadronic channels pass our cuts as often as the ρ channel, though of course a more detailed analysis should simulate more decay modes (including the three-prong modes). We estimate:

$$\sigma(t\bar{t}j \rightarrow \tau jjj b\bar{b} + \cancel{E}_T) = 0.09 \text{ fb} \quad (3.3)$$

In this and other τ -related backgrounds where all the \cancel{E}_T is from the decay $W \rightarrow \tau \nu \rightarrow j + \cancel{E}_T$, we have the advantage that the transverse mass $m_T(\mathbf{p}_T^j, \cancel{E}_T) < M_W$. Thus we do not have to reject every candidate event in which one of the jets reconstructs as a hadronic tau. We need only reject these events if they satisfy this transverse mass constraint. Thus, we have a *pessimistic* estimate of SM backgrounds (aside from possible mismeasurement backgrounds as discussed above).

The other backgrounds rely on higher fake rates or accidental mass reconstruction. They are small compared to $t\bar{t}Z$. We tabulate them in Table 1. Note that we have used Alpgen [27] to set a rough upper bound for the multi-jet processes.

⁴We will use “cross section” (denoted σ) loosely to mean cross section times branching ratio times relevant acceptances and efficiencies. That is, it is the quantity that when multiplied by luminosity gives the expected number of events passing all cuts. It includes our estimate of $\epsilon_{b\tau}$ for a given sample.

Channel	Generator	$\epsilon_{b\tau}$	σ
$t\bar{t}Z$ ($Z \rightarrow \nu\nu$)	MadGraph	0.18	0.32 fb
$t\bar{t}j \rightarrow \tau jjb\bar{b} + \cancel{E}_T$	MadGraph	0.011	0.09 fb
$t\bar{t}jj \rightarrow \tau\tau jjb\bar{b} + \cancel{E}_T$	MadGraph	0.0006	$\lesssim 10^{-5}$ fb
$Wb\bar{b} + 3j$ ($W \rightarrow \tau\nu$)	Alpgen	0.01	$\lesssim 0.009$ fb
$W + 5j$ ($W \rightarrow \tau\nu$)	Alpgen	3.5×10^{-6}	$< 10^{-5}$ fb
$Zb\bar{b} + 4j$ ($Z \rightarrow \nu\nu$)	Alpgen	0.18	$\lesssim 0.022$ fb
$Z + 6j$ ($Z \rightarrow \nu\nu$)	Alpgen	$6. \times 10^{-5}$	< 0.013 fb

Table 1: Cross section (times branching ratios times efficiencies) for backgrounds to the hadronic $t\bar{t} + 2N$ decays, after all cuts have been applied. In the Alpgen processes we have applied a subset of the cuts to get an upper bound. For the $W + jets$ processes we have not decayed the τ , so our estimate is very rough (the \cancel{E}_T comes solely from the ν_τ , but the hadronic tau decay involves other neutrinos).

3.5 Results for Significance and Signal to Background

Taking into account the various backgrounds and efficiencies we will now present our results for the discovery opportunities at the LHC. We will quantify the discovery opportunity in the usual way, after applying the cuts described in Section 3.2, of

$$\text{significance} = \frac{\text{signal}}{\sqrt{\text{background}}}, \quad (3.4)$$

where background is implicitly the number of background events from summing all backgrounds weighted with the appropriate efficiencies as found in Table 1, while signal is the number of signal events multiplied by the efficiency defined in Section 3. We will then discuss the signal to background ratio, as it will be important for future discussion as well as for giving another measure of discovery.

In Figure 1 we plot the discovery reach as defined by significance in (3.4) for a fermionic t' and scalar N for 10 fb^{-1} of integrated luminosity in the $m_{t'} - m_N$ plane. This plot will also be representative of the fermionic t' and vector N case since the overall rate of production is independent of the spin of the N . For the case of a fermionic t' we find that a large region of parameter space with only 10 fb^{-1} of luminosity allows for discovery. The maximum value for $m_{t'}$ of the contours exhibited in Fig 1 are essentially vertical in the $m_{t'} - m_N$ plane as the cross section roughly only depends on $m_{t'}$ for the bulk of the parameter space. When $m_{t'} \approx m_t + m_N$ interference effects start to become more important and the cross section decreases. The region where the interfering diagrams become important depends is somewhat sensitive to the coupling $g_{t'N}$ but it does have any significant impact for our study whatsoever for reasonable values of $g_{t'N}$.

For the case of a scalar t' the discovery reach is plotted for both 10 fb^{-1} and 100 fb^{-1} in Figure 2. For the case of a scalar t' we find that with only 10 fb^{-1} of luminosity the reach is only about 600 GeV which is lower than the fermionic t' case due to the smaller cross section for scalars. We find however that for an integrated luminosity of 100 fb^{-1} the reach in the scalar t' case is comparable to the fermionic case after 10 fb^{-1} .

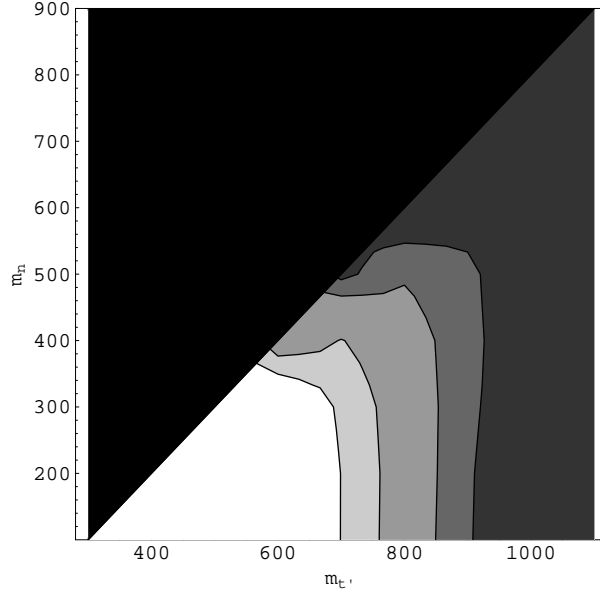


Figure 1: Significance of signal for t' fermion N scalar for 10 fb^{-1} . The contours (from left to right) represent significance of $> 15\sigma$, $> 10\sigma$, $> 5\sigma$, $> 3\sigma$, and $< 3\sigma$. The region $m_{t'} - m_N < 200 \text{ GeV}$ is not investigated.

While $\text{signal}/\sqrt{\text{background}}$ is the relevant quantity when attempting to understand if one has discovered physics beyond the Standard Model, the more interesting quantity for our purposes is $\text{signal}/\text{background}$. We are concerned not just with *discovering* new physics, but with *understanding* it. For that, we would like to have a clean sample of events that we understand to be mostly signal. This is especially important for studying angular distributions that help to determine the t' spin, as we will discuss in Section 5. There we will be looking for differences in the pseudorapidity distributions of top quarks. These already small differences will be diluted if a large number of background events are included. Having a clean sample of signal events will make the task much easier. We plot contours of signal to background ratio in Figure 3.

For relatively low t' masses, the sample is quite pure. For instance, for t' fermion at 300 GeV, N scalar at 100 GeV, the ratio $S/B \approx 70$. This low mass region is ideal; the cross section is high *and* the signal is very pure. On the other hand, at TeV-scale masses in the case of a fermionic t' or masses of about 700 GeV for a scalar t' , S/B approaches 1. In that case, it is very important to accurately understand *both* the signal and background cross sections and kinematic distributions. Given enough luminosity, at high masses the techniques we describe in Section 5 could still shed light on the t' spin, but to accurately understand the expected distributions one needs to understand how many of the events are signal and how many are background. For this one would ideally want NLL calculations of expected cross sections and kinematics, and also measurements of high- E_T top quark distributions in other channels to validate the calculations. Masses near a TeV are a difficult

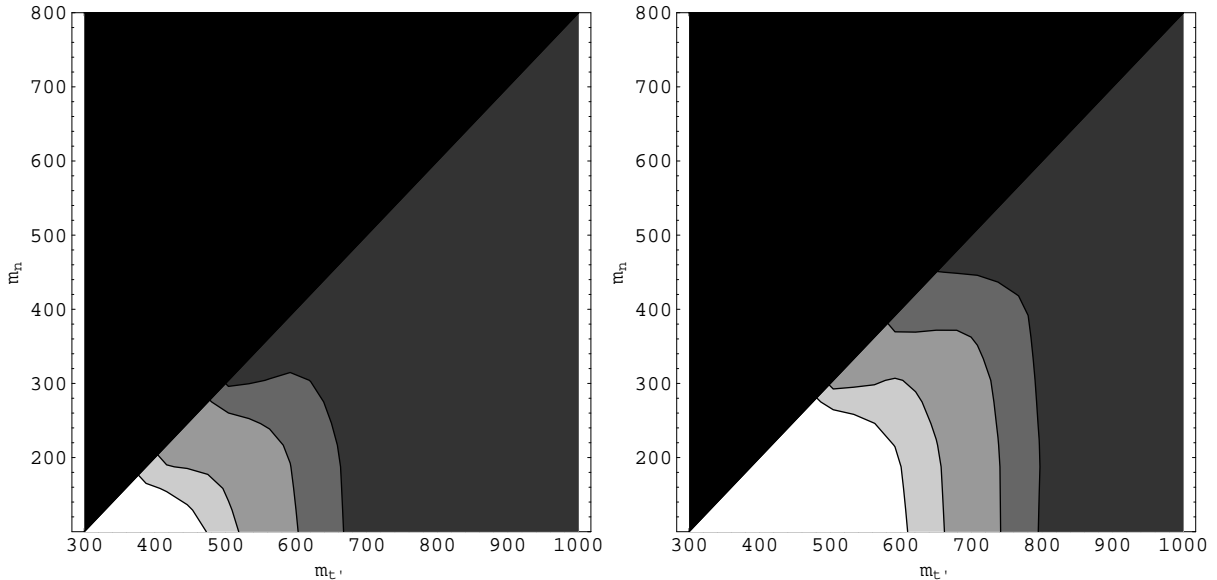


Figure 2: Significance of signal for t' scalar N fermion for 10 fb^{-1} on the left and 100 fb^{-1} on the right. The contours (from left to right) represent significance of $> 15\sigma$, $> 10\sigma$, $> 5\sigma$, $> 3\sigma$, and $< 3\sigma$. The region $m_{t'} - m_N < 200 \text{ GeV}$ is not investigated.

challenge both theoretically and experimentally. Still, there is a large region where S/B is large enough that background contamination is not a major worry. Our proposed techniques could be applied in a fairly straightforward way.

There are some foreseeable improvements of the analysis we have outlined that could improve performance in the region where background is neither negligible nor overwhelming. We have described a simple set of cuts that can be applied over a wide range of masses for the t' and N . Once one discovers new physics and gets a rough understanding of its mass scale, it might be possible to develop more sophisticated cuts to keep more of the signal relative to background. As just one example, consider the variable M_{T2} we described in Section 3.1. On a sample of pure $t'\bar{t}'$ events, M_{T2} will have an upper edge M_{T2}^{max} . If this sample is superimposed with background, the background events will have a smooth curve for M_{T2} lacking the upper edge. Thus a cut that $M_{T2} < M_{T2}^{max}$ will improve the signal purity. To understand how well this can work we would need a good detector simulation that accurately describes the smearing of the M_{T2} edge; precisely locating this edge may be difficult.

There are other instances where altering the cuts could help to increase the signal to background ratio. For instance, when $m_{t'} \approx m_t + m_N$, the decay products will generally be softer than in the typical point in parameter space. In this case one might relax the requirement that at least one jet have $E_T > 100 \text{ GeV}$, if it is possible to trigger on the events using some other requirement (e.g. high \cancel{E}_T and several high- E_T jets).

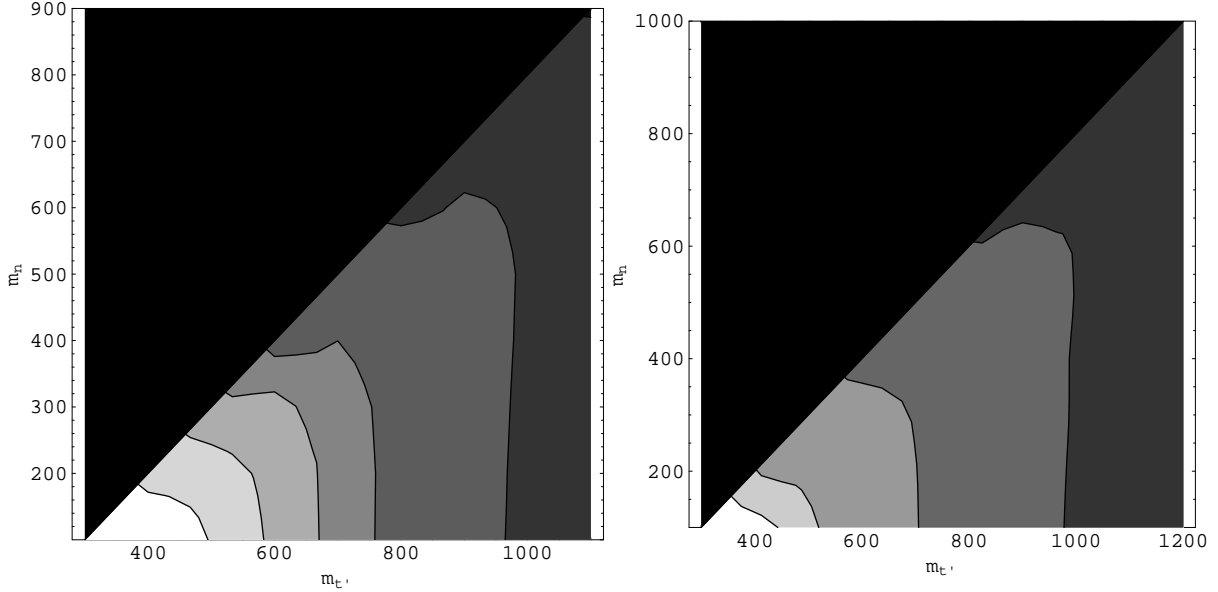


Figure 3: Signal to background plots. At left, the case t' fermion, N scalar. Contours (left to right) are $S/B = 40, 20, 10, 5, 1$. At right, the case t' scalar, N fermion. Contours are $S/B = 10, 5, 1, 0.1$.

4 Mass Determination

Once we have discovered a signal in $t\bar{t} + \cancel{E}_T$, the logical next step is to try to determine the mass of the t' and the N . This is complicated by the fact that we measure the two N 's only as missing transverse energy. Thus we measure $p_x^{N_1} + p_x^{N_2}$ and $p_y^{N_1} + p_y^{N_2}$ (without information to split the contributions of the two N 's) and we have no measure of the z components. On the other hand, in the top hadronic decay mode we can attempt to reconstruct the full four-momenta of the t and \bar{t} , by combining jets and demanding that each reconstruct to the top mass.

How can we use the kinematic information we have to measure the t' and N masses? On an event-by-event basis, it is apparent that we cannot. We simply do not have enough kinematic information to pin down a mass. On the other hand, with a large enough (and clean enough) sample of events we can use statistical techniques to measure the two masses. Our approach is to construct a number of variables that each are sensitive to the masses; if they have different contours in the $m_{t'} - m_N$ plane, then with enough of them we can get a good estimate of the two masses.

The first kinematic variables we consider are $\langle |\cancel{E}_T| \rangle$ and $\langle H_T \rangle$, where we average over all events passing our cuts. In general these increase with larger $m_{t'}$, and decrease with larger m_N (as m_N grows, more of the available energy goes to its mass and less to its p_T). We also consider the average $\langle M_{eff} \rangle$. Finally, we extract the kinematic edge $M_{T2}^{max}(m_{N;ref})$.

As it turns out, the variables $\langle |\cancel{E}_T| \rangle$, $\langle H_T \rangle$, $\langle M_{eff} \rangle$, and $M_{T2}^{max}(m_{N;ref})$ (for arbitrary

$m_{N;ref}$) do not give independent functions of $m_{t'}$ and m_N . This is demonstrated clearly by a contour plot in Fig. 4 (a). Each of these variables is giving an approximate measurement of the mass *difference* between the t' and the N . This observation was made independently recently in [8]. The noted success of M_{eff} in the mSUGRA context is due to the light neutralino mass there; in general M_{eff} does not depend strictly on the mass of the heavy colored particle but on some function of that mass and the mass of the LPOP.

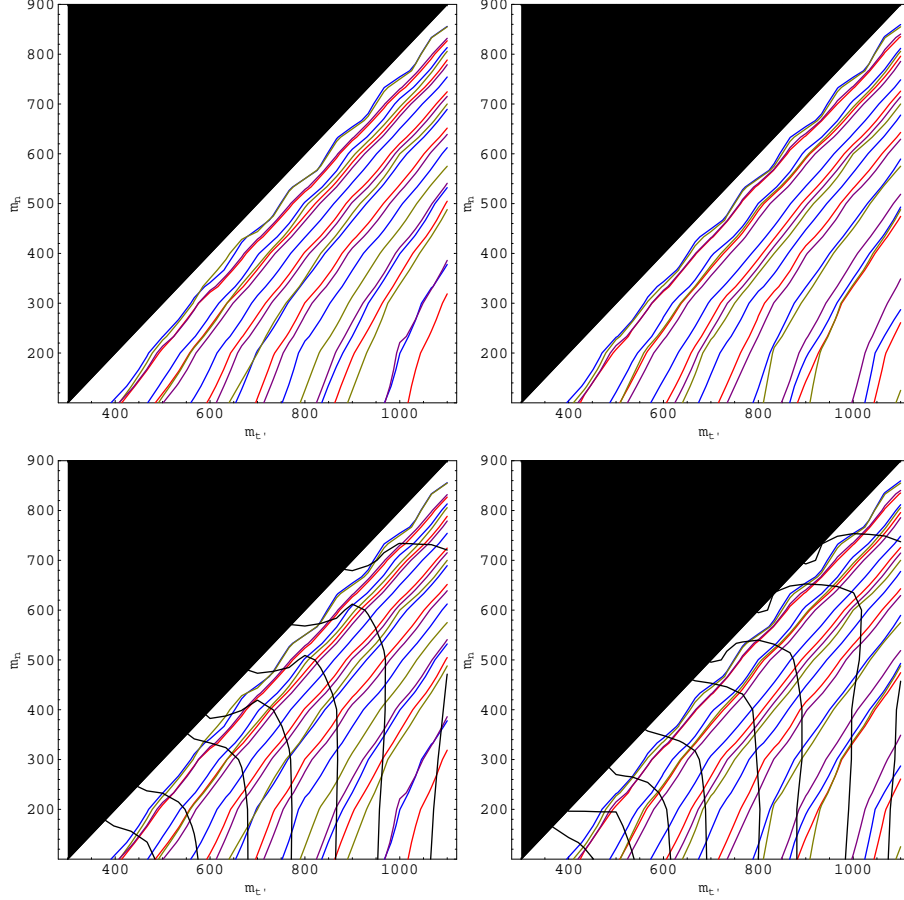


Figure 4: Top (a): contour plots of kinematic variables, demonstrating that they all measure the same function of $(m_{t'}, m_N)$. On the left is the case of t' fermion N scalar; at right, t' scalar N fermion. Bottom (b): the same plots, with contours of constant cross section superimposed. At left, t' fermion N scalar; at right, t' scalar N fermion. Approximately, the kinematic variables are all sensitive only to the mass *difference*, while the cross section is sensitive to the t' mass. ($\langle H_t \rangle$ is in red, $\langle |E_T| \rangle$ is in blue, $\langle M_{eff} \rangle$ is in purple, M_{T2}^{max} is in gold, and in (b) σ is in black.)

Since any of these variables measures only roughly a mass difference, they are insufficient to determine the two masses. On the other hand, for a given spin the overall cross section σ is sensitive mostly to the mass $m_{t'}$ of the top partner and depends strongly on m_N only

near the threshold for the decay $t' \rightarrow tN$. Thus a measurement of cross section and of another kinematic variable, say $\langle M_{eff} \rangle$, is sufficient to fix $(m_{t'}, m_N)$ for a given spin of the t' as shown in Fig. 4 (b). In general, we have a two-fold ambiguity from this measurement, as t' can be either a fermion or a scalar.¹ We refer to these as the non-SUSY and SUSY cases respectively. In the SUSY case, cross-sections are lower at a given mass, so for a given measured $(\sigma, \langle M_{eff} \rangle)$, the SUSY case corresponds to smaller masses. We will discuss below how to exploit this. For now, we note that given any SUSY point, there is a non-SUSY point with matching $(\sigma, \langle M_{eff} \rangle)$, obtained by raising both the t' and N masses. This translates to the fact that any point of the plot on the right hand side of Fig. 4 (b) is degenerate with a point in the plot on the left. On the other hand, the converse is not always true. For a given non-SUSY point, if $m_N \ll m_{t'}$, there will be no matching SUSY point. Once we reduce $m_{t'}$ to achieve the right σ , if the splitting measured by $\langle M_{eff} \rangle$ is larger than $m_{t'}$ then we cannot find an m_N to accommodate the SUSY case. Hence, it is conceivable that a simple measurement of cross section and effective mass can be inconsistent with SUSY. On the other hand, if such a measurement is consistent with SUSY, it is also consistent with the non-SUSY case and we need a new observable to split the degeneracy.

There are some caveats to the use of the cross section σ for mass determination, of course. For a given candidate $(m_{t'}, m_N)$ pair and spin, one can compute the expected σ , but this computation relies on the PDFs and on a good understanding of backgrounds and various efficiencies. There will be an inherent error in the determination of the mass given that the PDFs for gluons which will be the dominant channel at low x and quarks at higher x have large error bars. For instance the fractional error for the gluon PDF for x 's in the range of .1 and less are approximately 5% but rapidly increase for larger x [14]. Additionally one would need to understand the efficiency of the triggers relevant to this process since we are relying upon being able to really understand the actual number of events after reconstruction. The various efficiencies that are important for our study however should be better pinned down once a more complete understanding of the detectors is accomplished; however at most the result of this understanding will be to simply scale our cross sections by a number less than one but presumably very close to one given our conservative estimates. Despite the various concerns over the use of cross section, it is important to keep in mind that the dependence of the cross section on the t' mass is very strong so a large uncertainty on the cross section translates into a much smaller uncertainty on the t' mass. If there were a 100% error in the cross section it would be reflected as approximately a 100 GeV error in the bulk of our parameter space. For this reason we believe that even with the inherent uncertainties in the cross section measurement it can still be used for a reliable estimate of the masses.

The degeneracy we have pointed out, even after using cross section information to determine masses up to the choice of spin, is often not taken into account in recent studies attempting to distinguish SUSY and non-SUSY cases where the starting point is the same

¹We have checked that for t' a fermion, the cross section and kinematics are the same for N either scalar or vector. Here the coupling is fixed to be right-handed as in Equation 2.1, but these observables should be approximately the same for the more general coupling as in Equation 2.2. Preliminary checks confirm this, though there is some deviation that must be considered in understanding the theoretical errors on the measurement.

spectrum instead of the same cross sections and kinematic observables [9–12]. This is certainly a conceivable starting point given that one may be able to measure the spectrum independently in enough other channels, however from a bottom up perspective the degeneracy we demonstrate here seems more likely to be a concern if one is not in such an optimistic region as examined in other studies. It has been conjectured that with enough channels the ability to distinguish SUSY from a non-SUSY case is possible when looking at patterns of signatures, while any given channel can be made degenerate [11]. However, within the MSSM alone there are many degeneracies amongst parameters when looking at a large set of inclusive signatures [28], thus it is quite plausible to believe these degeneracies are no less frequent in the SUSY vs. non-SUSY cases especially given that new physics may not show up in multiple channels.

5 Spin Determination

We have seen that kinematic variables, together with cross section, are sufficient to give estimates of the masses $m_{t'}$, m_N for a *given choice* of spins, but that in general they do not distinguish the supersymmetric case from the non-SUSY case. To distinguish the various cases and also find the correct masses one has to find a method to distinguish the spins. There have been some attempts at coming up with techniques for spin determination at the LHC [9–12], however as mentioned before the starting point of these studies has been to choose an identical mass spectrum for a SUSY vs non-SUSY case. These studies do not break the degeneracy that we are interested in and thus do not distinguish the spins in the most general case. It is important to note though that given equivalent kinematics and cross section, the mass scale of the SUSY case is much lower. This is useful: we do not have to measure just spin correlations to distinguish the two cases. Instead, we can look for other quantities that distinguish the overall mass scale.¹

In general, spin correlations are studied by boosting to some optimal frame, choosing a plane, and then constructing some asymmetry from the distribution of decay products from the two original particles about the chosen plane. However, since we cannot resolve the direction of the two N particles, it is difficult to boost to a useful frame. The simplest thing that we can do is to try to build asymmetries in the lab frame, based on the momenta of the tops.

We define two candidate asymmetries:

- The **beam-line asymmetry** (BLA): Let p_z^{t1} and p_z^{t2} be the components of the top momenta along the beam-axis, in the lab frame. Define N_+^z to be the number of events where $p_z^{t1}p_z^{t2} > 0$ and N_-^z to be the number of events where $p_z^{t1}p_z^{t2} < 0$. Then our asymmetry is $BLA = (N_+^z - N_-^z)/(N_+^z + N_-^z)$. Equivalently, BLA can be defined based on the pseudorapidities of the tops, which have the same sign as p_z .

¹Of course, one might obtain information from other sources. For instance, determination of the N mass in a dark matter direct-detection experiment would allow us to obtain $m_{t'}$ from $M_{T2}^{max}(m_N)$, and then we could simply read off the t' spin from the cross section as suggested in [10, 11, 29]. However, we will be pessimistic and assume we must learn everything from the $t\bar{t} + \cancel{E}_T$ signal.

- The **directional asymmetry** (DA): Consider $\cos \theta_{t\bar{t}}$ where $\theta_{t\bar{t}}$ is the angle between the top momenta in the lab frame. In general the cross section will have a linear dependence on $\cos \theta_{t\bar{t}}$, but isolation cuts remove the events where this is near 1. We define N_+^d as the number of events where $0.5 < \cos \theta_{t\bar{t}} < 0.9$ and N_-^d as the number of events where $-0.9 < \cos \theta_{t\bar{t}} < -0.5$. Our asymmetry is $DA = (N_+^d - N_-^d)/(N_+^d + N_-^d)$.

These asymmetries convolve effects of spin correlations and of overall mass scale. We have listed them for a variety of points with similar kinematics and cross section in Table 2. They are both consistently larger in the SUSY case. For the BLA, it is particularly easy to understand how the mass scale affects the quantity we compute, since the BLA can be defined using only pseudorapidities. First consider the SUSY case. We produce two scalar tops, so there can be no initial spin correlation. In the center-of-mass frame of the colliding partons, the stops are back-to-back. Each stop decays isotropically in its rest frame. Thus, in the center-of-mass frame of the colliding partons, the two tops have a higher probability of moving in opposite directions with respect to a given plane than of moving in the same direction. In the case of a fermionic t' , the expected asymmetry is modified, because the spins of the initial $t'\bar{t}'$ pair are correlated. In either case, the center-of-mass frame differs from the lab frame by some overall boost along the beam axis. The parton distribution functions are rapidly falling functions of x , so at heavier masses one should expect a smaller average boost. On the other hand at lower masses the boost will often be large enough that the BLA becomes significantly greater than zero. In this way the BLA will give some indication of the x values of the colliding partons. This is clear in Table 2; for a given spin, the asymmetry falls off at higher masses.

In addition to these asymmetries, there is a related technique for studying the effect of the mass scale on the observed data. We have noted that the BLA can be defined in terms of pseudorapidity. It is instructive to study the pseudorapidity distributions of the two tops directly. The difference $\eta_- = \eta_1 - \eta_2$ is invariant under boosts along the beam axis, but the sum $\eta_+ = \eta_1 + \eta_2$ is not. We plot events for the different spin cases in the (η_+, η_-) plane in the figure 5, for a pair of points with matching cross section and kinematics. It appears that to a good approximation the events are Gaussian distributed in the two variables. In this way the distributions define an ellipse; in the scalar case, this ellipse is stretched out significantly more on the η_+ axis. The observation that the scalar case is more stretched out when looking at a particular degeneracy is obviously commensurate with the results of the BLA and DA. The additional use of the information related to η_- has been argued to be sensitive only to spin correlation [12] in certain cascade decays. This again was studied in the context of a degenerate mass spectrum thus avoiding the degeneracies associated with different mass scales. When investigating the degeneracies we presented in Section 4 it is almost impossible to entirely deconvolve the effects of mass scale and spin correlation. That is why we advocate the asymmetries as well as the full correlation in pseudorapidity where both the η_+ and η_- information are useful, and depending on the masses involved one may have a much stronger effect at distinguishing the spins.

To quantify the results of pseudorapidity correlations, we perform a likelihood fit for the

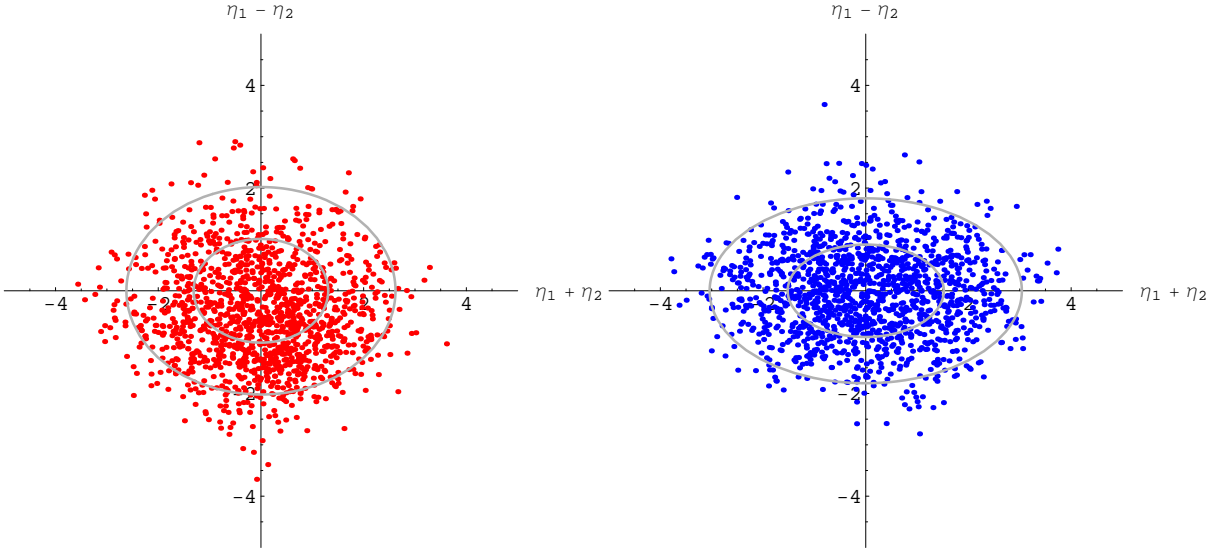


Figure 5: Distribution of events in the (η_+, η_-) plane for two points with similar cross-section and kinematics but different spins, with one and two sigma contours. At left: t' fermion, mass 700 GeV, N scalar, mass 400 GeV, $(\sigma_+, \sigma_-) = (1.31, 1.01)$; at right, t' scalar, mass 500 GeV, N fermion, mass 150 GeV, $(\sigma_+, \sigma_-) = (1.52, 0.90)$. In the lighter (t' scalar) case, there is on average more boost, so the ellipse is stretched more along the η_+ axis.

standard deviations σ_+ and σ_- , maximizing $-2 \log \mathcal{L}$ where $\mathcal{L} = \prod_i P(\eta_{+i}, \eta_{-i})$ with

$$P(\eta_+, \eta_-) = \frac{C}{\sigma_+ \sigma_-} \exp \left(-\frac{\eta_+^2}{2\sigma_+^2} - \frac{\eta_-^2}{2\sigma_-^2} \right). \quad (5.1)$$

The likelihood fit was performed using Minuit [30]. Minuit returns errors on the fitted parameters σ_+ and σ_- . These errors should scale like $1/\sqrt{N_{events}}$, and this is consistent with the samples of unweighted events we have analyzed. The coefficient, as reported by Minuit, is approximately 1.² We view the Minuit errors as approximately describing the experimental error after a given number of events, though other effects must be considered. (For instance, finite η resolution will have some effect, although if the smearing of the η 's of the two tops is uncorrelated it does not seem that it should pose major problems for our fit.)

As an example, consider the degeneracy of t' fermion at 700 GeV and N scalar at 400 GeV with t' scalar at 500 GeV and N fermion at 150 GeV. The corresponding fitted values of σ_+ are 1.31 and 1.52 respectively. The cross section (with all branching ratios and efficiencies taken into account) is about 2.0 fb. Ignoring background (which is a factor of 5 smaller),

²Obtaining large numbers of *unweighted* events to systematically explore the error on various random subsamples is computationally intensive, but on a variety of samples up to 7,000 events we obtain error estimates ranging from $0.93/\sqrt{N_{events}}$ to $1.04/\sqrt{N_{events}}$.

one will have about 600 signal events after 300 fb^{-1} , and $1/\sqrt{N_{\text{events}}}$ is ≈ 0.04 . Taking this to be a good measure of the error, at this point the fitted values are separated by 5σ . With about 1200 fb^{-1} of luminosity, the fitted values are separated by 10σ . Here we are restricting ourselves to considering the right-handed coupling Eq. 2.1. If we allow a more general Lorentz structure, there might be some small range around these fitted values allowed for a given choice of t' spin, so one will want to pick the most pessimistic separation, and the luminosity required might be somewhat larger. (Unless some additional measurement can help fix the Lorentz structure of the coupling.) Similar considerations will apply to BLA and DA, and to σ_- , which grows smaller in the scalar case. One can measure each of these quantities for more consistency, but they are highly correlated, so they do not give independent checks of the t' spin.

Of course, how confidently one can say a measured set of data corresponds to one case or the other will depend on the measured central value. Given the possibility that mismeasurement and other considerations will lead to the actual efficiency being somewhat less than our estimates, we think it best to be cautious rather than make a definitive claim about the luminosity needed to distinguish spins. Ultimately a detailed study with detector simulation, larger samples, and inclusion of background together with signal is necessary to understand exactly the scope of applicability of this technique, but it appears promising. It appears that with several hundred fb^{-1} up to a few thousand fb^{-1} one can use angular observables to resolve the spin of the t' over a wide range of masses. Making this discrimination could require the LHC luminosity upgrade [31]. It is interesting to note that the LHC may be more feasible for spin determination than a linear collider dependent on the values of $m_{t'}$; future study of this is worth investigating.

6 Relevance To General Scenarios

We have focused exclusively on the signature $t\bar{t} + \cancel{E}_T$. In most models of new physics there will be additional new physics states accessible at the LHC. It is important to ask whether our discussion is still applicable in such cases. Signatures from other new states will, of course, provide other clues to the underlying model, but they also could potentially make the analysis we have outlined more difficult. There are multiple sources of complication: new backgrounds, new decay modes, and new production channels. Our method should be applicable in a wide variety of cases, despite the added complications.

In a model with additional parity-odd states, there are potentially new backgrounds to our signal. The most obvious is an additional (somewhat heavier) parity-odd top. In SUSY, for instance, one always expects two scalar tops, from the mixing of the partners of t_L and t_R . This is clearly a background that we cannot eliminate by harder kinematic cuts. However, it should be relatively straightforward to deal with in many scenarios. If the additional parity-odd top is so heavy that its cross section is well below that of the lightest t' , we can ignore it when performing our analysis. If it is light enough that it has a significant cross section (well above SM backgrounds), then it would show up on the M_{T2} plot as a second edge. By the relative location and height of the two edges, one could possibly learn the difference in

mass and in cross section of the two parity-odd tops. This is a case where M_{T2} could give us clear new information, and deserves further study. The most troublesome case would be very nearly degenerate partners of the t_L and t_R , since they would be nearly indistinguishable but would increase the overall cross section. This requires further study.

As another example involving new parity-odd states, a sufficiently heavy parity-odd Z' might decay to $t' + \bar{t}$, for instance. Production of $Z'N$, then, would give $t\bar{t} + \cancel{E}_T$. This would be quite difficult to distinguish from our signal, but the cross section should be smaller due to the weak couplings involved in the production, and there is some branching fraction $Br(Z' \rightarrow t'\bar{t})$ multiplying this cross section as well.

New parity-even states can also give backgrounds to our signal. For instance, in the Littlest Higgs with T-parity one can have a T-even top t'_+ that has some branching fraction to $t'N$. Single production of t'_+ is the dominant channel, but it is generally produced in association with a light-quark jet. Pair production of t'_+ would fake our signal, and could happen in the low-mass region. If the branching fraction and cross section are large enough that this fakes our signal at a high rate (implausible in the Littlest Higgs with T-parity, but possible since we are thinking model-independently), one should consider the use of M_{T2} to find an additional edge as we discussed for the extra odd t' .

Less directly, long decay chains could provide events with multiple jets and \cancel{E}_T . As with Standard Model backgrounds, if actual tops are not produced, cuts on mass reconstruction and b -tagging will remove much of such backgrounds. However, some backgrounds could be more troublesome. For instance, in SUSY one could have $\tilde{g}\tilde{q}$ with $\tilde{g} \rightarrow \tilde{t}t$. Vetoing additional hard jets could be useful in such events, but one needs a good understanding of pile-up, initial state radiation, and other issues that could lead to additional jets in the signal itself. Whether these cuts will be sufficient for a clean $t'\bar{t}'$ sample will depend on the details of the mass spectrum under consideration, but it is plausible that we can reject most of the backgrounds without sacrificing too much efficiency on the signal. On the other hand, an ATLAS study of a particular mSUGRA point found that it was difficult to obtain a very pure sample of $\tilde{t}\bar{\tilde{t}}$ production over SUSY backgrounds [17, 20]. Again, this is a case where intelligent use of M_{T2} might provide useful new information, and much will depend on the details of the spectrum.

Another consideration is that in a more complicated model, the t' is likely to have other decay channels. For instance, one might consider $W'b$, Wb' , $Z't$, or $Z'c$. In general these will have similar signatures to our tN decay: for instance, $W'b \rightarrow jjbN$, but the $j\bar{j}b$ mass will no longer be constrained to equal the top mass. To measure the branching fractions one wants to try to find each of these modes, but the lack of mass window cuts implies that they are more susceptible to multi-jet SM backgrounds. This deserves further study. If all the decay channels can be measured reasonably well, one can estimate the branching fraction to tN and apply our analysis. So long as the $t' \rightarrow tN$ branching fraction is $\mathcal{O}(1)$, and new physics backgrounds do not swamp the signal, one should still be able to apply our analysis. (Of course, more luminosity might be needed.)

A further consideration in the presence of other new physics is that new production channels might open up for the t' . For instance, a relatively light gluino in SUSY would alter the production cross section. Thus, to apply our analysis of mass determination using cross

section, one would need some idea of how much the cross section is altered by the other new physics. However, as we have noted, even large uncertainties in the cross section translate to relatively small uncertainties in masses. It seems unlikely that new physics will cause large differences in cross section, so this might not be very problematic.

There is much more work to be done to understand how further details of the model can complicate an analysis of the sort we have outlined. However, it appears that in a large variety of models $t' \rightarrow tN$ is a significant decay mode that can be observed cleanly. Once new physics is observed in several channels, one can start to understand how the uncertainties in our analysis are affected. The claim that at the same mass scale scalar top cross sections are significantly smaller than fermionic t' cross sections is a robust one, and we expect that the LHC can discriminate the two spins in a wide variety of models. It is also worth pointing out that new physics might not be described by any current model. It is conceivable that new physics will have a relatively light t' with no other states light enough to affect our results.

7 Conclusions

In this paper we have put forth a new perspective for studying the phenomenology of physics beyond the SM that directly relates to the LHC. We have advocated a model independent signature based analysis motivated by naturalness to develop new tools, and we have hopefully dispelled certain misconceptions. We have begun utilizing this new methodology by analyzing the first new particle dictated by naturalness, the partner of the SM top quark, t' .

Based on the model independent framework that we set up in this paper of having a parity odd t' decay to a right handed top quark and the lightest parity odd particle N we set out to answer the following questions:

- Can the signature be observed at high significance over the SM backgrounds?
- How well can we determine the masses of the t' and N ?
- Can we devise an algorithm for measuring the spin of the t' or the N ?

We have shown that in the hadronic channel for a large range of t' mass the t' has a large significance and can be discovered at the LHC within a short running time. We additionally demonstrated over a large range of t' mass the ratio of signal to background is greater than 1. We then set up a program for measuring the masses of t' and N . We showed that standard kinematic observables measure only one independent function of $m_{t'}$ and m_N , which is approximately the mass *difference* over much of parameter space. Additionally we demonstrated that certain kinematic observables that have been used in the past to determine the mass of strongly interacting particles are only justified in certain regions. The way we found most effective for measuring both the mass of t' and N was to combine any standard kinematic observable with the cross section. We found though that this *only* determines the masses up to a discrete choice of spin. Given a scalar t' (SUSY case) there always is a corresponding fermionic t' (non SUSY) with a heavier mass that has the same kinematic observables. This degeneracy is not accounted for in many studies comparing models where

the starting point is often to choose the same mass spectrum. To break the degeneracy we needed to determine spin information from the LHC. We introduced several possible ways to break the spin degeneracy. Most promising was using the additional kinematic information about the rapidities of the top quark in the hadronic channel. We put forth a new asymmetry as well as studying correlations amongst rapidities that can be used to determine the spin of t' , and thus pin down the masses of the particles. This can be taken heuristically as a way to determine the difference between SUSY and other models.

There are several logical extensions to our work. In focusing on the top sector we have narrowed the scope of our study to discovery possibilities and determination of basic properties such as mass and spin. If naturalness is really playing a role in TeV scale physics one would need to test this by determining the couplings of the t' to the Higgs. One could also extend our study to an even more generic coupling to the top quark as well as including a partner of the bottom quark. From this bottom up model independent point of view a logical next step would also be to add in more particles dictated by naturalness, i.e. partners of the SM gauge bosons and Higgs. We leave these possibilities as well as others that can be motivated from the philosophy set forth in this paper for future study.

Acknowledgments

We thank Ulrich Heintz, Meenakshi Narain, Peter Onyisi, Maxim Perelstein, and Matt Strassler for useful conversations. We thank Adam Aurisano and Seth Zenz for directing us to useful references on related experimental issues. We thank Fabio Maltoni and Tim Stelzer for answering MadGraph questions. PM would like to thank the theory groups at Boston University, Harvard University, and the University of Washington for their hospitality while this paper was in preparation. PM and MR were supported in part by the National Science Foundation under grant PHY-0355005 and MR was supported by a National Science Foundation Graduate Research Fellowship.

References

- [1] N. Arkani-Hamed, A. G. Cohen, E. Katz and A. E. Nelson, JHEP **0207**, 034 (2002) [arXiv:hep-ph/0206021].
- [2] G. R. Farrar and P. Fayet, Phys. Lett. B **76**, 575 (1978).
- [3] S. Dimopoulos and H. Georgi, Nucl. Phys. B **193**, 150 (1981). N. Sakai and T. Yanagida, Nucl. Phys. B **197**, 533 (1982). S. Dimopoulos, S. Raby and F. Wilczek, Phys. Lett. B **112** (1982) 133.
- [4] H. C. Cheng and I. Low, JHEP **0309**, 051 (2003) [arXiv:hep-ph/0308199], H. C. Cheng and I. Low, JHEP **0408**, 061 (2004) [arXiv:hep-ph/0405243], I. Low, JHEP **0410**, 067 (2004) [arXiv:hep-ph/0409025].

- [5] T. Appelquist, H. C. Cheng and B. A. Dobrescu, Phys. Rev. D **64**, 035002 (2001) [arXiv:hep-ph/0012100].
- [6] H. C. Cheng, K. T. Matchev and M. Schmaltz, Phys. Rev. D **66**, 056006 (2002) [arXiv:hep-ph/0205314].
- [7] J. Hubisz and P. Meade, Phys. Rev. D **71**, 035016 (2005) [arXiv:hep-ph/0411264].
- [8] H. C. Cheng, I. Low and L. T. Wang, arXiv:hep-ph/0510225.
- [9] A. J. Barr, Phys. Lett. B **596**, 205 (2004) [arXiv:hep-ph/0405052], M. Battaglia, A. K. Datta, A. De Roeck, K. Kong and K. T. Matchev, arXiv:hep-ph/0507284, A. Datta, K. Kong and K. T. Matchev, arXiv:hep-ph/0509246,
- [10] J. M. Smillie and B. R. Webber, arXiv:hep-ph/0507170,
- [11] A. Datta, G. L. Kane and M. Toharia, arXiv:hep-ph/0510204.
- [12] A. J. Barr, arXiv:hep-ph/0511115.
- [13] F. Maltoni and T. Stelzer, JHEP **0302**, 027 (2003) [arXiv:hep-ph/0208156], T. Stelzer and W. F. Long, Comput. Phys. Commun. **81**, 357 (1994) [arXiv:hep-ph/9401258], H. Murayama, I. Watanabe and K. Hagiwara, KEK-91-11
- [14] J. Pumplin, D. R. Stump, J. Huston, H. L. Lai, P. Nadolsky and W. K. Tung, JHEP **0207**, 012 (2002) [arXiv:hep-ph/0201195].
- [15] M. Beneke *et al.*, arXiv:hep-ph/0003033.
- [16] I. Hinchliffe, F. E. Paige, M. D. Shapiro, J. Soderqvist and W. Yao, Phys. Rev. D **55**, 5520 (1997) [arXiv:hep-ph/9610544].
- [17] ATLAS Collaboration TDR Vol. 1. CERN-LHCC-99-14, ATLAS Collaboration TDR Vol. 2. CERN-LHCC-99-15
- [18] C. G. Lester and D. J. Summers, Phys. Lett. B **463**, 99 (1999) [arXiv:hep-ph/9906349], A. Barr, C. Lester and P. Stephens, J. Phys. G **29**, 2343 (2003) [arXiv:hep-ph/0304226].
- [19] T. Schörner-Sadenius, S. Tapprogge, *et. al.* ATLAS Note ATL-DAQ-2003-004.
- [20] G. Polesello, L. Poggioli, E. Richter-Was, J. Söderqvist, ATLAS Note PHYS-No-111, October 1997.
- [21] U. Baur, A. Juste, D. Rainwater and L. H. Orr, arXiv:hep-ph/0512262.
- [22] S. Eidelman *et al.* [Particle Data Group], Phys. Lett. B **592**, 1 (2004).
- [23] D. Cavalli and S. Resconi, ATLAS Note ATL-PHYS-98-118 (1998).

- [24] Pretty Good Simulator,
<http://www.physics.ucdavis.edu/~conway/research/software/pgs/pgs.html>
 Tuned for the LHC as per the LHC Olympics version.
- [25] T. Sjostrand, L. Lonnblad, S. Mrenna and P. Skands, arXiv:hep-ph/0308153.
- [26] R. Arnowitt et. al., <http://hepr8.physics.tamu.edu/hep/stau/susytalkd.pdf>
- [27] M. L. Mangano, M. Moretti, F. Piccinini, R. Pittau and A. D. Polosa, JHEP **0307**, 001 (2003) [arXiv:hep-ph/0206293].
- [28] N. Arkani-Hamed, G. L. Kane, J. Thaler and L. T. Wang, arXiv:hep-ph/0512190.
- [29] M. Battaglia, A. Datta, A. De Roeck, K. Kong and K. T. Matchev, JHEP **0507**, 033 (2005) [arXiv:hep-ph/0502041].
- [30] F. James and M. Roos, Comput. Phys. Commun. **10**, 343 (1975).
- [31] F. Gianotti *et al.*, Eur. Phys. J. C **39**, 293 (2005) [arXiv:hep-ph/0204087].

Spin (t', N)	$(m_{t'}, m_N)$	$\langle H_t \rangle$	σ	BLA	DA	σ_+	σ_-
(F,S)	(550,300)	781	5.1	0.22	-0.43	1.40	1.05
(S,F)	(390,115)	786	5.0	0.31	-0.25	1.59	0.94
(F,V)	(550,300)	779	5.2	0.22	-0.46	1.39	1.03
(F,S)	(600,350)	775	3.3	0.16	-0.44	1.38	1.15
(S,F)	(415,165)	777	3.1	0.32	-0.34	1.57	0.82
(F,V)	(600,350)	785	3.4	0.20	-0.46	1.37	1.00
(F,S)	(650,350)	860	3.1	0.16	-0.41	1.35	0.99
(S,F)	(475,100)	863	2.9	0.30	-0.23	1.53	0.92
(F,V)	(650,350)	860	3.2	0.19	-0.40	1.34	1.05
(F,S)	(700,400)	865	2.0	0.16	-0.40	1.31	1.01
(S,F)	(500,150)	874	2.1	0.26	-0.32	1.52	0.90
(F,V)	(700,400)	857	2.1	0.16	-0.45	1.30	1.08
(F,S)	(700,500)	695	0.51	0.19	-0.66	1.27	1.03
(S,F)	(515,315)	742	0.44	0.36	-0.55	1.40	0.75
(F,V)	(700,500)	690	0.50	0.17	-0.64	1.20	0.94
(F,S)	(750,425)	904	1.6	0.15	-0.39	1.32	1.00
(S,F)	(550,150)	917	1.5	0.21	-0.23	1.51	0.93
(F,V)	(750,425)	896	1.6	0.14	-0.37	1.30	1.05
(F,S)	(800,450)	943	1.2	0.13	-0.34	1.28	1.07
(S,F)	(575,125)	956	1.2	0.24	-0.24	1.45	0.97
(F,V)	(800,450)	936	1.2	0.13	-0.34	1.30	1.03
(F,S)	(900,500)	1019	0.66	0.087	-0.29	1.25	1.11
(S,F)	(645,60)	1043	0.68	0.15	-0.22	1.45	1.08
(F,V)	(900,500)	1012	0.66	0.12	-0.32	1.28	1.11
(F,S)	(900,550)	953	0.59	0.11	-0.36	1.23	1.07
(S,F)	(645,235)	967	0.61	0.20	-0.26	1.41	1.04
(F,V)	(900,550)	947	0.60	0.13	-0.38	1.26	1.07

Table 2: Asymmetries and rapidity ellipse shapes for points with matching kinematics. Masses and H_t in GeV, σ in fb. S denotes spin 0, F denotes spin 1/2, V denotes spin 1. These numbers are reported for *signal only*; for the points with lower cross section, one needs to consider the effect of the background on the measured quantities. Signal becomes diluted at high masses, so discriminating among the spins grows more difficult.